

Reduction of Error Measurements for an Accurate 3-D Reconstruction in Biplane Cineangiography

Farida Cheriet, Jean Meunier

Université de Montréal, département d'informatique et de recherche opérationnelle
P.O. Box 6128, Station Centre-ville, Montréal (Canada), H3C 3J7.

Jacques Lespérance

Institut de Cardiologie de Montréal, 5000 Bélanger, Montréal (Canada), H1T 1C8.

Abstract

The purpose of this paper is to elaborate a 3D reconstruction method, using X-ray angiograms acquired daily by the clinician, without any special calibration procedure during the X-ray examination. The absolute geometry of the X-ray imaging system is determined by an iterative procedure based on the minimization of the mean square distances between observed and predicted projections of a set of reference points (≥ 12) identified by the clinician on a simultaneous pair of images. Once the geometry of the imaging system has been found, the 3D structure of interest is retrieved from classical methods of binocular stereovision. The method should be particularly useful in clinical applications since it needs very little intervention from the clinician. The method could also be of interest in other applications of stereovision such as robotics.

Résumé

La reconstruction 3D de structures vasculaires en cinéangiographie biplan a suscité d'importantes recherches en imagerie médicale. Les méthodes existantes ont l'inconvénient d'être fondées sur l'utilisation d'un objet de calibration. Nous proposons une approche originale pour la détermination de la géométrie absolue du système d'acquisition d'images à partir d'appariements ponctuels identifiés par un radiologue sur une paire simultanée d'images. Cette approche est basée sur une procédure itérative d'approximation non linéaire destinée à minimiser la distance quadratique moyenne entre les projections analytiques et observées de l'ensemble des points de référence identifiés. Cette méthode peut être très utile dans des applications cliniques vu qu'elle nécessite un minimum d'intervention de la part du clinicien et permet une reconstruction précise de la structure 3D à partir de deux séquences d'images de routine acquises par des systèmes non calibrés.

1. Introduction

Intensive efforts have been made to reconstruct the 3D coronary arteries from biplane angiograms to improve their structure analysis. Several workers have reported techniques that utilize biplane digital angiographic images obtained in exactly orthogonal directions [1]. However the relative orientation of the two views must be completely flexible in order to give a good visualization of the vascular structures of interest in both images. Therefore, in practice conventional techniques for quantitative determination of 3D object structure from biplane images require the use of a calibration phantom [2,3]. Despite the demonstrated feasibility of these techniques they have not found wide-spread clinical use because the physician usually considers that the use of a calibration phantom would disturb the already quite complex clinical protocol. Several investigators working outside the field of medical imaging [4,5,6,7,8] have reported the basis of a technique that allows 3D object structure to be determined from biplane images obtained at arbitrary relative orientations without the use of a calibration phantom. L.E.Fencil et al. [9] have described the theoretical aspects of the approach as it applies to biplane radiography. Their method requires the matching of at least eight coronary bifurcation points of unknown 3-D location on a pair of views. Unfortunately the approach depends on the *exact* knowledge of some geometrical parameters of the biplane system to recover the absolute values of the 3-D structure. In this paper, we describe an iterative procedure to determine the absolute geometry of the biplane X-ray imaging system that has the advantage of only requiring *estimations* of the geometrical parameters involved.

2. Problem statement

2.1. Angiographic images

The X-ray system basically consists of an X-ray source and an image intensifier with a camera which can be moved around the patient. The clinician positions the camera in order to give a good visualization of the vascular structure of interest. The direction of the camera according to the patient is specified by two angles, the right-left and the caudal-cranial angulations. In biplane X-ray imaging the patient is surrounded by two sets of X-ray tube and image intensifier. Biplane coronary angiography is taken from two different directions, the R.A.O (right anterior oblique) and L.A.O (left anterior oblique) views, as shown in fig.1. The values of the caudal-cranial and the right-left angulation are chosen by the clinician according to the morphology of the heart and the stature of the patient.

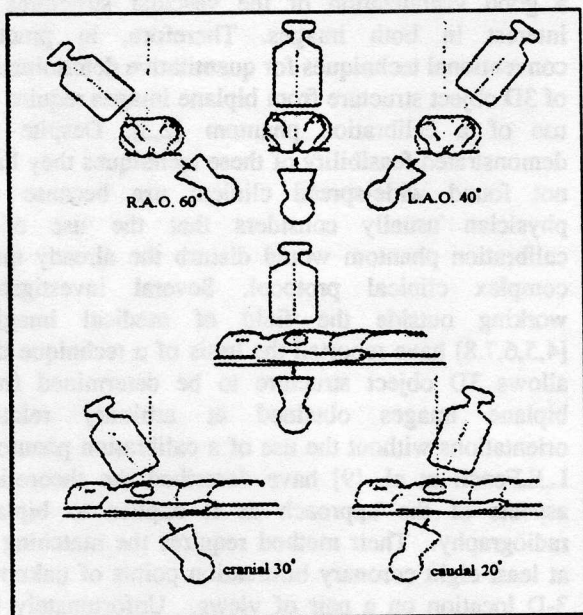


Fig.1. Position of the image intensifier according to the patient

2.2. Geometry of the biplane X-ray imaging system

The different coordinate systems used in our approach are described by fig.2. Let $R=(O,X,Y,Z)$ be the object coordinate system, the origin O is defined as the intersection point of the projection axis

of the left and the right systems; the existence of this point is always assured when clinicians position a biplane X-ray system because they carefully align them so that the projection axis of the left and the right systems meet at the middle of the left ventricle, in order to provide optimum images of the entire coronary tree. However, the origin position remains undefined until the clinician adjusts the biplane X-ray system (no prior knowledge of the isocenter position). The X-axis and Y-axis refer respectively to right-left and caudal-cranial directions of the patient; the Z-axis refers to posterior-anterior direction which is the vertical to the patient. Let S_1, S_2 denote respectively the position of the two X-ray sources and $R_1=(S_1, x_1, y_1, z_1), R_2=(S_2, x_2, y_2, z_2)$, their associated coordinate systems where the zx planes are respectively parallel to the corresponding uv image planes. For a biplane X-ray system, the perspective projection of a 3-D object point onto the left and right image planes can be modeled as two linear transformations in homogeneous coordinates with 3×4 matrices M_1 and M_2 representing respectively the calibration matrices of the left and right systems.

$$\begin{aligned} [\omega_i \cdot u_i \quad \omega_i \cdot v_i \quad \omega_i]^t &= M_i \cdot [X \quad Y \quad Z \quad 1]^t \\ \text{for } i &= 1, 2 \end{aligned} \quad (1)$$

Where ω is a scaling factor, and (u, v) are the image coordinates of a 3-D point (X, Y, Z) .

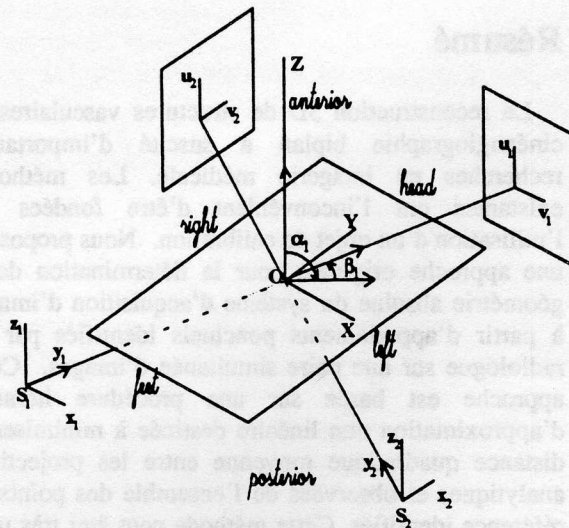


Fig.2. Definition of the coordinate systems

The classical calibration method [2,3] consists of estimating the elements of the matrices M_i for $i=1,2$ by solving the linear system obtained from known 3-D coordinates of at least 6 non-coplanar reference points.

2.3. Self-calibration of the biplane X-ray imaging system

In our approach, we make *explicit* use of the description of the calibration matrices with the geometrical parameters of the biplane X-ray system. Thus the matrices M_i can be decomposed as follows:

$$M_i = P(d_i, s_p, u_{S_i}, v_{S_i}) D_i \quad \text{for } i=1,2 \quad (2)$$

Where s_p denotes the known pixel size, d_i is the distance from the source S_i to the image plane, (u_{S_i}, v_{S_i}) are the image coordinates of the source S_i projection, and the matrix P represents the linear transformation in homogeneous coordinates associated with the perspective projection of a 3-D point on the image plane. D_i is the matrix describing the displacement from the object coordinate system $R = (O, X, Y, Z)$ to the source coordinate system $R_i = (S_i, x_i, y_i, z_i)$. The relationship between the coordinates (x_i, y_i, z_i) of a point in R_i and the coordinates (u_i, v_i) of its 2-D projection, are given by:

$$\begin{cases} (u - u_{S_i}) s_p = z_i \cdot d_i / y_i \\ (v - v_{S_i}) s_p = x_i \cdot d_i / y_i \end{cases} \quad \text{for } i=1,2$$

These relations may be written in matrix form

$$\begin{bmatrix} \omega_i u_i & \omega_i v_i & 0 & \omega_i \end{bmatrix}^t = P(d_i, s_p, u_{S_i}, v_{S_i}) \begin{bmatrix} x_i & y_i & z_i & 1 \end{bmatrix}^t$$

for $i=1,2$

with :

$$P(d_i, s_p, u_{S_i}, v_{S_i}) = \begin{bmatrix} 0 & u_{S_i}/d_i & 1/s_p & 0 \\ 1/s_p & v_{S_i}/d_i & 0 & 0 \\ 0 & 0 & 0 & 0 \\ 0 & 1/d_i & 0 & 0 \end{bmatrix}$$

for $i=1,2$

The transformation required to align the object coordinate system R with the source coordinate system

R_i is defined by the adjustment done by the clinician to position the X-ray camera according to the patient. As shown in fig.2, there is first an α rotation around the Y-axis to achieve the right-left angulation, and a β rotation around the X-axis to achieve the caudal-cranial angulation, and finally a translation of d_{S_i} along the Y-axis from the origin O to S_i . This leads to the following expression of D_i :

$$D_i = T_Y(d_{S_i}) \cdot R_X(\beta_i) \cdot R_Y(\alpha_i) \quad \text{for } i=1,2$$

Using equation (2), the calibration matrices are decomposed as follows:

$$M_i(\xi_i) = P(d_i, s_p, u_{S_i}, v_{S_i}) \cdot T_Y(d_{S_i}) \cdot R_X(\beta_i) \cdot R_Y(\alpha_i) \quad \text{for } i=1,2 \quad (3)$$

with :

$$\xi_i = (\alpha_i, \beta_i, d_i, d_{S_i}, u_{S_i}, v_{S_i})$$

The calibration of the biplane X-ray imaging system consists of estimating the geometrical parameters $(\xi_i)_{i=1,2}$ of the system. For this purpose, the mean square distance between observed and analytical projection of a set of N reference points of *unknown* 3-D coordinates is minimized to provide the better estimate $\xi^* = (\xi_1^*, \xi_2^*)$. The coordinates of the analytical projection $(u_{ni}(\xi_i, X_n, Y_n, Z_n), v_{ni}(\xi_i, X_n, Y_n, Z_n))_{i=1,2}$ of an object point (X_n, Y_n, Z_n) can be derived from equation (1). The clinician identifies the approximate position of several suitable landmarks such as artery branching points that can be located in both biplane images. Afterwards, the exact position in both views are found automatically and the observed projection coordinates $(u_{ni}, v_{ni})_{i=1,2}$ of the reference points in each view, are measured to the nearest pixel. The criterion which must be minimized to estimate the geometrical parameters $\xi = (\xi_1, \xi_2)$ follows:

$$\begin{aligned} \varepsilon(\xi, L) = & \frac{1}{N} \sum_{n=1}^N \sum_{i=1}^2 (u_{ni} - u_{ni}(\xi_i, X_n, Y_n, Z_n))^2 \\ & + (v_{ni} - v_{ni}(\xi_i, X_n, Y_n, Z_n))^2 \end{aligned}$$

with: $L = ((X_1, Y_1, Z_1), (X_2, Y_2, Z_2), \dots, (X_N, Y_N, Z_N))$, the *unknown* 3-D coordinates of the reference points. The

method employed to solve this minimization problem is iterative and requires an initial guess for each unknown parameter. To choose reasonable initial guesses for the geometrical parameters we take advantage of the measurements registered from the gantry control circuit of the X-ray imaging system, during image acquisition. Knowing the initial geometric parameters ξ^0 , the initial three-dimensional coordinates L^0 of the reference points are derived from the accurately measured image coordinates (u_i, v_i) in both views, by applying equations (1) and (3). At the r^{th} iteration the parameters (ξ^r, L^r) are updated by computing the corrections $\Delta = (\Delta\xi, \Delta L)$, and the updated parameters $(\xi^r + \Delta\xi, L^r + \Delta L)$ are used as approximations for the next iteration. The whole iteration process is repeated until the corrections Δ or the criterion $\varepsilon(\xi, L)$ become negligible. The algorithm developed for this purpose is described by the diagram shown in fig. 3.

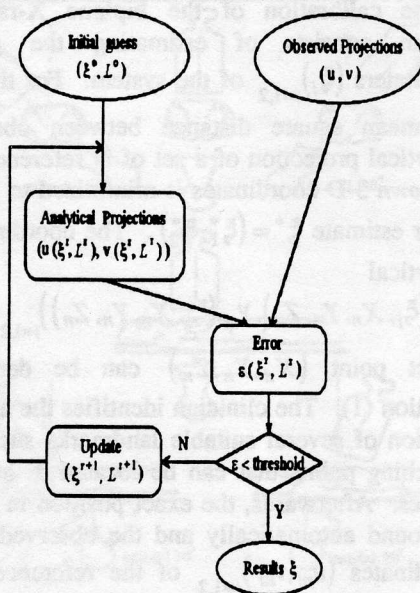


Fig.3. Self-calibration algorithm

The computation of the correction $\Delta = (\Delta\xi, \Delta L)$ can be performed using numerical methods. We have found that the modified finite difference Levenberg-Marquardt algorithm described elsewhere [10,11,12], converge to a reasonable estimate when a set of at least 12 reference points is considered.

3. Simulation of biplane X-ray images of the coronary tree

The simulation experiment consists of the following two steps:

1. A predetermined number of infinitesimal object points ($N \geq 12$) are generated within the common volume of the biplane imaging system. The object points are placed on the surface of an ellipsoid of 20 cm major axis and 10 cm minor axis, that is centered on the point at which the y_1 and the y_2 axes intersect. The object points are linked to simulate the 3-D coronary tree shown in fig. 4.

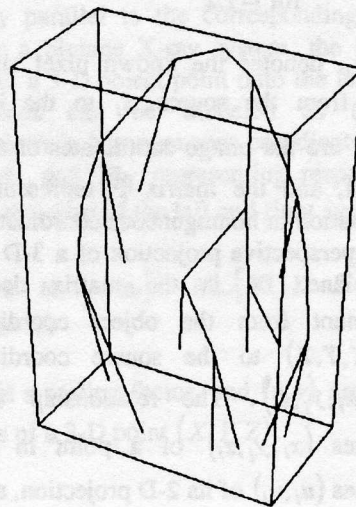


Fig.4. Simulation of a 3-D tree

2. Several parameters must be specified to define the biplane imaging geometry. The size of the image receptor and the number of pixels in two orthogonal directions determine the effective pixel size of the system. We assumed a 17.8x17.8 cm square image receptor, a 512x512 pixel image matrix, and thus a pixel size $s_p = 0.035$ cm as in Fencil et al.[9]. The perpendicular distances between the two sources and their respective image planes are set to $d_1 = d_2 = 100$ cm. We assume that the y_1 and y_2 axes intersect at $y_1 = 0.5 d_1$ and $y_2 = 0.5 d_2$, thus $d_{S1} = d_{S2} = 50$ cm. The angle values α_i and β_i are varied to simulate different incidences which generally interest the clinician. Once the biplane imaging geometry is specified, the exact image coordinates of each object point in each view, (u_{n1}, v_{n1}) and (u_{n2}, v_{n2}) are

calculated. The left ($\alpha_1=\pi/3, \beta_1=\pi/6$) and right ($\alpha_2=5\pi/6, \beta_2=\pi/6$) projections of the 3-D tree simulated in fig. 4 are shown in fig.5.

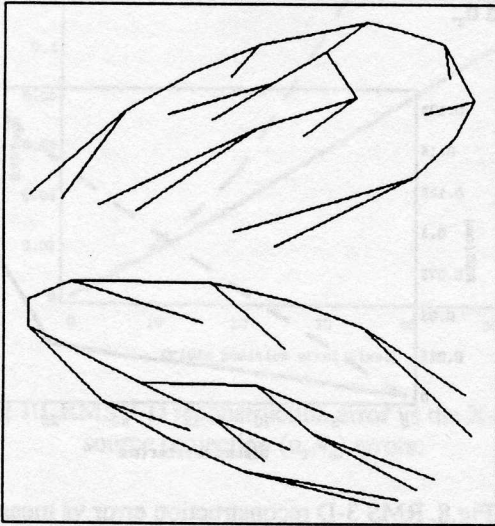


Fig.5. The simulated 3-D tree Projections

coordinates. The comparison is performed by computing the root mean square (RMS) distance between the original and the reconstructed bifurcation point positions. The 3-D reconstruction of the simulated tree under perfect conditions is almost perfect as expected, with an RMS error of 3×10^{-15} cm. This small error is due to the floating-point arithmetic imprecision of the computer during the process of projection and backprojection.

4.2. Effects of errors in the initial geometrical parameters

To simulate the unavoidable inaccuracies of the measured parameters we introduce an error in each geometrical parameter ($\pm\pi/30, \pm 10$ cm, ± 10 pixels for angles, distances and 2-D coordinates respectively). To assess the effects of this error on the 3-D reconstruction process, the 3-D simulated tree is first retrieved from its two projections and the erroneous geometrical parameters. Fig. 5 shows the non-corrected 3-D reconstructed tree superposed on the original simulated tree.

4. Results

4.1. Accuracy of the method in perfect conditions

The principal goal of the self-calibration is to determine the absolute geometry of the imaging system in order to recover the 3-D structure of interest from its right and left projections. To examine the inherent ability of the technique to recover 3-D information, we first performed the computations under perfect conditions. To this end, the image coordinates (u_i, v_i) of the 3-D tree bifurcation points, simulated in section 3, are computed exactly (infinite resolution), rather than simply to the nearest pixel, and no measurement errors are introduced on the initial *geometrical* parameters. Arbitrarily, a biplane geometry is selected with the following characteristics:

$$\xi_1 = (\pi/3, \pi/6, 100, 50, 0, 0) \text{ and}$$

$$\xi_2 = (5\pi/6, \pi/6, 100, 50, 0, 0)$$

Once the 3-D tree is retrieved from its two projections, the 3-D coordinates of the reconstructed 3-D tree bifurcation points are compared with the original

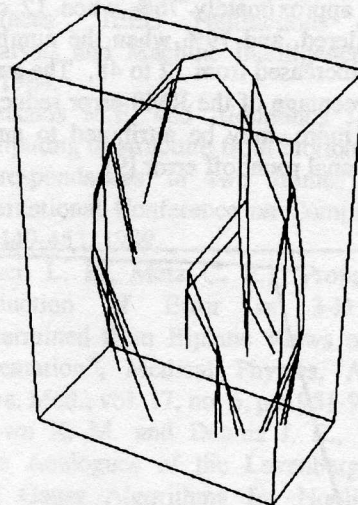


Fig.5. Superposition of the non-corrected reconstruction on the simulated 3-D tree

Afterwards the proposed algorithm is applied to correct the erroneous geometrical parameters. Fig.6 shows the 3-D reconstructed tree (after the correction process) superposed to the original simulated tree. Notice that contrary to the algorithm developed by Fencil et al.[9] where the 3-D coordinate estimates can differ by a translation, rotation and/or scale factor

from the true ones, our method gives directly the real absolute values of these 3-D coordinates.

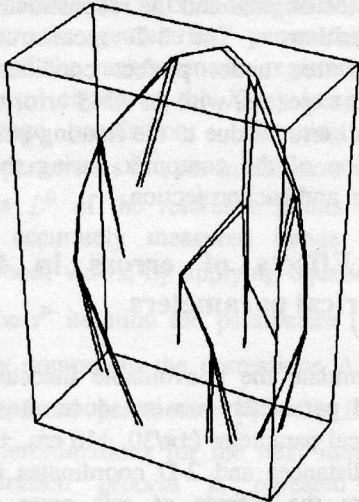


Fig.6. Superposition of the corrected reconstruction on the simulated 3-D tree

To examine the stability of the 3-D reconstruction process, the RMS error is computed by varying the number of matched points identified on a pair of images. Fig.7. shows that the initial average error drops by approximately 76% when 12 object points are considered, and 79% when the number of object points is increased from 12 to 48. The small decrease in the percentage of the RMS error reduction when N increases more, may be attributed to an increase in computational roundoff error [9].

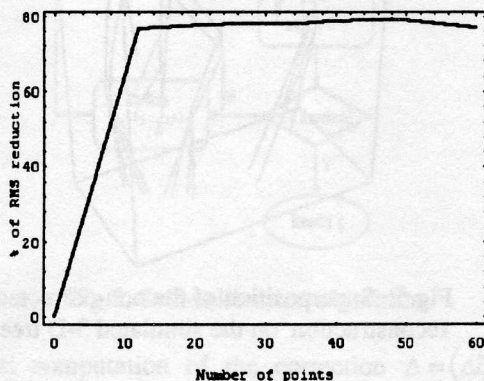


Fig.7. RMS 3-D reconstruction error vs number of reference points.

To assess the effects of errors in the measured distances d_1 and d_2 , we introduced positive or negative errors of up to 30 cm in both distances. The propagation of these errors on the accuracy of the

reconstruction process is illustrated by the dashed curve shown in Fig.8. The solid curve in shows the ability of our approach to correct these errors. Thus, for the conditions studied here, we conclude that our approach is effective for errors of less than 30 cm in d_1 and d_2 .

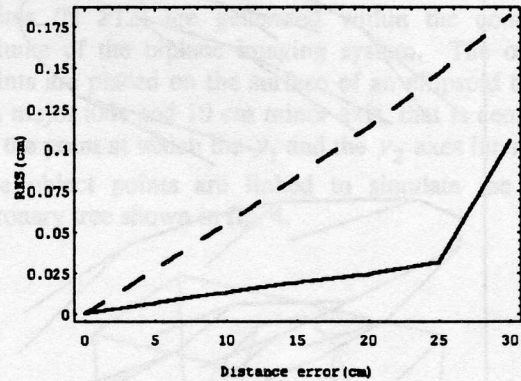


Fig.8. RMS 3-D reconstruction error vs measured distances

The effects of error in the measured angles on the 3-D reconstruction error is shown in Fig.9. The dashed curve illustrates the propagation of these errors on the accuracy of the reconstruction process. The continued curve shows that our approach reduces substantially the effect of these errors, for the particular views considered.

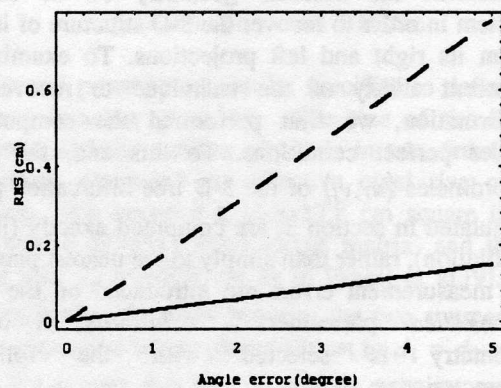


Fig.9. RMS 3-D reconstruction error vs measured angles.

We also simulated combinations of positive and negative errors in the 2-D coordinates (u_s, v_s) of the source projection on both views. Fig.10. shows that

errors of up to 50 pixels do not affect noticeably the accuracy of the reconstruction process. These results can be explained by noting that 50 pixels in the image plane corresponds to 1.75 cm in the 3-D world.

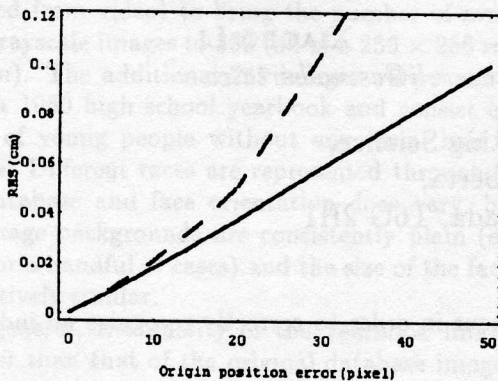


Fig.10. RMS 3-D reconstruction error vs the X-ray source projection (u_s, v_s) errors.

5. Conclusion

This work demonstrates the feasibility of an accurate 3D reconstruction, using only the projection coordinates of matched points in a pair of images, without a prior knowledge of the exact geometry of the imaging system. For clinical applications the clinician identifies the approximate locations of a minimum of 12 suitable artery branching points on a pair of images, and establish correspondence between the reference points. Afterwards the exact position of each branching point is found automatically. Using the exact position of the projection coordinates of the reference points, our method determines the absolute geometry of the system in order to retrieve the coronary 3D structure of interest. We believe that this approach will be useful to better investigate arterial tree abnormalities. The method could also be of interest in other applications of stereovision such as robotics.

References

- [1] Tran L.V., Bahn R.C., and Sklansky J., "Reconstructing the Cross Sections of coronary Arteries from Biplane Angiograms", IEEE Transactions on Medical Imaging 1992.
- [2] Saito T., Misaki M., Shirato K., Takishima T., "Three-Dimensional Quantitative Coronary Angiography", IEEE Transactions on Biomedical Engineering, vol. 37, no. 8, pp. 768-777, 1990.
- [3] Rougée A., Picard C., Ponchut C., and Troussset Y., "Geometrical Calibration of X-ray Imaging Chains for Three-Dimensional Reconstruction", Computerized Medical Imaging and Graphics, vol. 17, nos. 4/5, pp. 295-300, 1993.
- [4] Haralick R.M., Joo H., Lee C. N., Zhuang X., Vaidya V. G., and Kim M. B., "Pose Estimation from Corresponding Point Data", IEEE Transactions on Systems, Man, and Cybernetics, vol. 19, no. 6, pp. 1426-1445, 1989.
- [5] Trivedi H. P., "A Semi -analytic Method of Determining Stereo Camera Geometry from Matched Points in a Pair of Images : Coincident Meridional Planes, Exact or Noisy Data", Computer Vision, Graphics, and Image Processing, vol. 51, pp. 299-312, 1990.
- [6] Luong Q. T., Faugeras O., "Self Calibration of a Stereo Rig from Unknown Motions and Point Correspondences", INRIA Institute, Report N-2014, 1993.
- [7] Tsai R.Y. and Huang T.S., "Uniqueness and estimation of three-dimensional motion parameters of rigid objects with curved surfaces", IEEE Transactions on Pattern Analysis and Machine Intelligence, 6, pp.13-27, 1984.
- [8] Spetsakis M.E. and Aloimonos J., "Optimal computing of structure from motion using point correspondences in two frames", In Proc. International Conference on Computer Vision, pp.449-453, 1989.
- [9] Fencil L. E., Metz C. E., "Propagation and Reduction of Error in 3-D Structure Determined from Biplane Views of Unknown Orientation", Medical Physics, Am. Assoc. Phys. Med., vol. 17, no. 6, pp. 951-961, 1990.
- [10] Brown K. M. and Dennis J. E., "Derivative Free Analogues of the Levenberg-Marquardt and Gauss Algorithms for Nonlinear Least Squares", Numer. Math., vol. 18, pp. 289-297, 1972.
- [11] Levenberg K., "A method for the Solution of Certain Non-Linear Problems in Least Squares", Quart. Appl. Math., vol. 2, pp. 164-168, 1944.
- [12] Marquardt D. W., "An Algorithm for Least-squares Estimation of Nonlinear Parameters", J. SIAM, vol. 11, no. 2, 1963.